Computers and Concrete, *Vol. 22, No. 1 (2018) 27-37*
DOI: https://doi.org/10.12989/cac.2018.22.1.027

A numerical-experimental evaluation of beams composed of a steel frame with welded and conventional stirrups

Wagner L. Gonçalves[*2], Guilherme F. Gomes[1a], Yohan D. Mendéz[1b], Fabrício A. Almeida[3c], Valquíria C. Santos[4d] and Sebastião S. Cunha Jr.[1e]

[1]*Mechanical Engineering Institute, Federal University of Itajubá (UNIFEI), Avenue BPS, 1303, Itajubá, Brazil*
[2]*University Center of the Guaxupé Educational Foundation (UNIFEG), Avenue Dona Floriana, 463, Guaxupé, Brazil*
[3]*Institute of Industrial Engineering and Management, Federal University of Itajubá (UNIFEI), Avenue BPS, 1303, Itajubá, Brazil*
[4]*Institute of Natural Resources, Federal University of Itajubá (UNIFEI), Avenue BPS, 1303, Itajubá, Brazil*

(Received December 13, 2017, Revised April 11, 2018, Accepted April 12, 2018)

Abstract. Reinforced concrete structures are widely used in civil engineering projects around the world in different designs. Due to the great evolution in computational equipment and numerical methods, structural analysis has become more and more reliable, and in turn more closely approximates reality. Thus among the many numerical methods used to carry out these types of analyses, the finite element method has been highlighted as an optimized tool option, combined with the non-linear and linear analysis techniques of structures. In this paper, the behavior of reinforced concrete beams was analyzed in two different configurations: i) with welding and ii) conventionally lashed stirrups using annealed wire. The structures were subjected to normal and tangential forces up to the limit of their bending resistance capacities to observe the cracking process and growth of the concrete structure. This study was undertaken to evaluate the effectiveness of welded wire fabric as shear reinforcement in concrete prismatic beams under static loading conditions. Experimental analysis was carried out in order compare the maximum load of both configurations, the experimental load-time profile applied in the first configuration was used to reproduce the same loading conditions in the numerical simulations. Thus, comparisons between the numerical and experimental results of the welded frame beam show that the proposed model can estimate the concrete strength and failure behavior accurately.

Keywords: cracks; finite element method; nonlinear concrete; prismatic beam; steel frame; welded stirrups

1. Introduction

Reinforced concrete (RC) is one of the most widely used materials in civil and industrial engineering applications due to the fact that it is highly resistant and can be easily modeled for wide variety of different formats (Mosoarca and Victor 2013, Haifeng and Jianguo 2009). This variety has resulted in concrete being one of the most widely consumed materials in the world, according to Aïtcin (2000), and as such, its quality must be continually improved. Modern reinforced concrete structures need to be designed not only to withstand normal impact loads, such as weight, but also more significant impact loads, such as earthquakes and explosions (Haifeng and Jianguo 2009). Several studies are focused on the research surrounding reinforced concrete, such as: Saw *et al.* (2017), Yelgin *et al.* (2014), Lin *et al.* (2013), Han *et al.* (2011), Haifeng and Jianguo (2009). In addition to this, companies are continually seeking to adapt to new technologies and methodologies in waste reduction, minimizing cost without sacrificing quality.

Different concrete structures may have specific characteristics represented by the more resistant parts of their construction, these parts which seek to absorb and transmit forces, if they seek to maximize safety and the integrity of a building.

Notably, according to Fan and Hu (2013), reinforced concrete is made up of diverse combinations of materials, presenting forms of traction reinforcement. In addition to this, Fan and Hu (2013) state that many authors have contributed several theoretical and experimental studies on the quality of reinforced concrete, such as Colajanni *et al.* (2014), Azad *et al.* (1989), Ruiz *et al.* (1998), Ferro *et al.* (2007), Shaowei *et al.* (2011), in which they used experimental techniques, linear elastic fracture mechanics, acoustic emissions, among others, to verify fracture problems in reinforced concrete.

Research on reinforced concrete structures is often directed towards the feasibility of the execution of a project, with the primary concerns being saving material and manpower. Reinforced concrete structures constitute civil works of great responsibility, which call for confidence in

*Corresponding author, Professor
E-mail: wagner1709@mail.unifeg.edu.br
[a]Professor
E-mail: guilhermefergom@unifei.edu.br
[b]Ph.D. Student
E-mail: yohan.g8@unifei.edu.br
[c]Ph.D. Student
E-mail: fabricio-almeida@unifei.edu.br
[d]Professor
E-mail: valquiria@unifei.edu.br
[e]Professor
E-mail: sebas@unifei.edu.br

http://www.techno-press.org/?journal=cac&subpage=8
ISSN: 1598-8198 (Print), 1598-818X (Online)

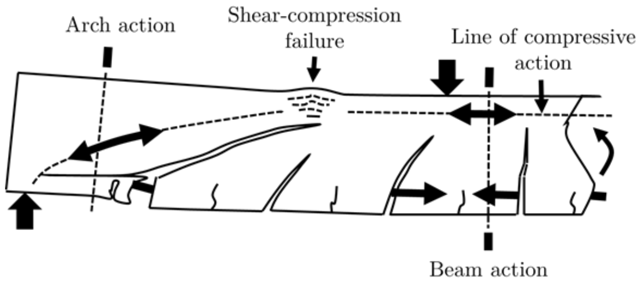

Fig. 1 Rupture by shear-traction (Shehdeh 2015)

the dimensioning of the pieces, quality in the material to be used, and great care in the execution of the project. Concrete is a material that has a high resistance to compression tension, however it displays low resistance to traction, hence the need to attach material with high tensile strength to the concrete, i.e., steel, which is intended to withstand tensile stresses. The quality of reinforced concrete can be verified through tests such as shear failure in RC elements, which was used in several works such as: Nielsen (1984), Vecchio and Collins (1986), Collins *et al.* (1996), Russo and Puleri (1997), Russo *et al.* (2004).

Shear cracks caused by loads upon beams are caused by the trellis effect, wherein the shear reinforcements rupture and crack, and/or crack by shear force-traction upon reaching their tensile strength. Thus, the most common type of shear failure occurs at the location where the beam is divided into two parts, and where it is secured only by the transversal anchorage. The use of this anchorage can bring about an element of safety to the structure. Fig. 1 shows the concrete shear and its anchorage.

It is equally important to point out that the main objective of this article is to compare the structural performance of reinforced concrete beams using welded and lashed frames, while mainly seeking an experimental quantitative and qualitative approach to the performance of the frames in their various configurations, numerical results for the welded frame beam samples is also provided. To do this the behavior of normal and tangential stresses, up to the limit state of resistant capacity of reinforced concrete beams with different moorings, will be compared: i) frames with welded stirrups and ii) frames with conventionally tied stirrups with annealed wire. After developing and manufacturing these two frame configurations a four-point bending test was carried on the samples. From the results it was possible to develop numerical models for the welded frame beam via Finite Element Method (FEM).

According to Dawari and Vesmawala (2014), numerical and finite element data modeling favors structural analysis of reinforced concrete beams, since this method divides a structure into non-superimposed parts of finite size and quantity.

Finite elements are interconnected by nodal points, or nodes, so this method transforms a continuous solid into an association of discrete elements. Compatibility and equilibrium equations are given for the nodes that unite them. The internal stresses and deformations of the elements are determined by interpolating the obtained results at each of the nodes, thus allowing for the definition of the stress state for the whole element, where each of these elements is suitable for different types of applications of materials and structures. There are many studies that use the finite element method applied to reinforced concrete, citing research such as: Markou and Papadrakakis (2013) which use the finite element method to simulate nonlinear behavior of reinforced concrete structures to predict nonlinear behavior in the experiments, comparing numerical predictions with real data and literature. In a paper published by Marzec *et al.* (2013), quasi-static numerical simulations were performed to evaluate the behavior of short beams of reinforced concrete without shear reinforcement, showing mixed shear stress from the finite element method. Colajanni *et al.* (2014) apply the finite element method to analyze an ideal model of ordinary reinforcement in pre-stressed concrete beams. In research conducted by Altunişik *et al.* (2013), the finite element method was used for modal analytical and experimental analyses for bridges in order to analyze their dynamic characteristics, such as natural frequency, for example. There are several other works that use numerical modeling techniques, such as FEM applied to research on reinforced concrete, as in: Lykidis and Spiliopoulos (2014), Javidan *et al.* (2014), Gürsoy (2014), Kaklauskas and Ghaboussi (2001), Ibraheem *et al.* (2014), Cosgun and Sayin (2014), Türker and Bayraktar (2014), Zhu *et al.* (2014), Hossain and Okeil (2014), Zhou *et al.* (2014).

Several studies were developed in order to compare different stirrups configurations, as in: Colajanni *et al.* (2014), Khan *et al.* (2015), Shatarat *et al.* (2016), on the other hand other authors as: Alam and Hussein (2012), Ulzurrun and Zanuy (2017) guide their researches in order to evaluate the effect no shearing reinforcement (without stirrups) in beams. To the best of our knowledge, most of the comparative assessments in reinforced concrete beams is done between configurations taking into account a called “reference beam” which does not include a reinforced frame or at least without stirrups, as previously mentioned and welded or conventional stirrups, but comparisons between these last configurations are not common in the literature, except for the work of Deivanai and Sathia (2016) in which was made a comparative study between them but without a numerical validation. In the present work the numerical verification of the displacement behavior and the good agreement between the numerical and experimental results for the welded frame RC beam represents one of the main contributions.

This manuscript is organized in the following manner: section 2 consists of a general bibliographic review, which addresses the techniques and theories used in the study. The methodological procedure is also presented in this section. Section 3 presents the numerical and experimental results of the concrete welded stirrup beam application, detailing the design, steps, and results. Finally section 4 draws the conclusions.

2. Numerical modeling and experimental procedure

2.1 Concrete steel frame

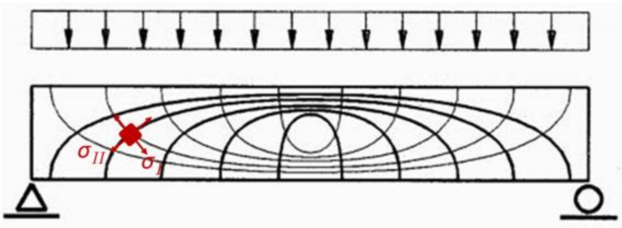

Fig. 2 Trajectory of the principal stresses of a bi-supported beam

For Fusco (2007), there is a step-by-step process for calculating reinforced concrete beams. The first calculation refers to the determination of the longitudinal reinforcement for the maximum bending moments, followed by the calculation of the transverse reinforcement for resistance to the shear forces. Several models were developed for the analysis of reinforced concrete beams under shear force, however, the lattice model has been the most widely used due to its simplicity and practicality.

Furthermore, two models of calculation for transversal reinforcement are permitted in the Brazilian standard NBR 6118/2014. The first model is called the Model of Calculus I, and the second Model of Calculus II. The classic Ritter-Mörsch truss is adopted in the first model, while the second allows for a model called “generalized truss”. Over the last decades more refined models have been presented, such as the Rotating angle softened truss model (RA-STM), the fixed angle softened truss model (FA-STM), and the “Truss model with crack friction”, which considers the friction between the surfaces of the inclined cracks and models based on compression fields.

According to Bastos (2015), under these circumstances the development of an inclined crack by shearing force (a crack that increases up near to the upper edge of the compressed zone of the concrete) depends on the stiffness to the deformation of the trapezoid, otherwise, the weaker the trammel, the more it lengthens with increasing load, and the faster the inclined crack becomes dangerous. Also, having a slip of the anchor in the bearing has a weakening effect, and thus both influences must be taken into account with constructive details in the execution of the armature.

The behavior of the transverse reinforcing beams is highly influenced by the distribution of the stirrups. As the main inclined tensile stresses reach the concrete's tensile strength, the first inclined cracks appear perpendicular to the direction σ_I, as shown in Fig. 2. The fissures arise, redistribution of the internal forces occurs, and the transverse reinforcement and compressed diagonals then “work” more effectively. This redistribution is dependent upon the amount and direction of the transverse reinforcement (Leonardard and Mornning 1982).

If the transverse reinforcement is insufficient, the steel reaches the beginning of flow deformation (ε_y), and the biases close to the support develop rapidly toward the compressed limb due to the shear force, reducing its resistant section, which can then break abruptly as shown in Fig. 3. The absence of transverse reinforcement can also lead to this form of rupture. The crack propagates along the longitudinal tensile reinforcement in the vicinity of the bearing, separating it from the rest of the beam.

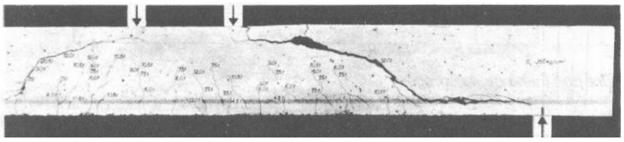

Fig. 3 Breaking of beam and slab by rupture of upper compressed concrete batten (Leonhardt and Monning 1982)

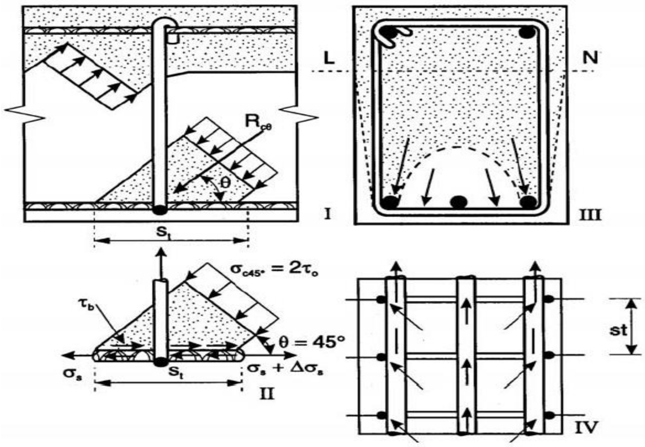

Fig. 4 Actuation of the stirrup in a truss model (Fusco 2000)

It should be noted that the existence of transverse reinforcement modifies the behavior of the beams after the inclined cracks appear, and which occur in the vicinity of the supports. Upon being intercepted by the fissure, the stirrups then transfer the tensile stresses between the two sides of the fissure. There is also a reserve of strength, provided mainly by the friction at the interface of the crack, due to the engagement between the concrete parts. The stirrups contribute to a ductile rupture as they continue to flow.

Equally important, according to Bastos (2015), considering beams with a high transverse reinforcement rate, rupture can occur due to the crushing of the compressed concrete of the inclined diagonals, after the formation of inclined cracks, as part of the additional shear force must be transferred by the aforementioned mechanisms. By increasing the crack opening, the friction at the interfaces decreases, which then leads to an increase in the force transferred by the concrete from the compressed batten and pin action, until the compressed concrete crushes or ceases the action of the pin.

Fig. 4 shows the work developed by the vertical stirrup in the trellis analogy for a beam with traction in the lower fiber. At the lower vertices the stirrup interweaves the traction longitudinal reinforcement, and at the top vertices the stirrup is anchored in the concrete of the compressed batten and in the upper longitudinal reinforcement.

The lower horizontal branch of the stirrups is important because, in addition to supporting the connecting rods, it also acts to balance the tensile stresses arising from the transverse slope of the diagonal connecting rods, as indicated in Fig. 4, III and IV. Fig. 4 II shows the support of the connecting rod at the intersection of the stirrup with the lower longitudinal bar, and the increase in tension in the

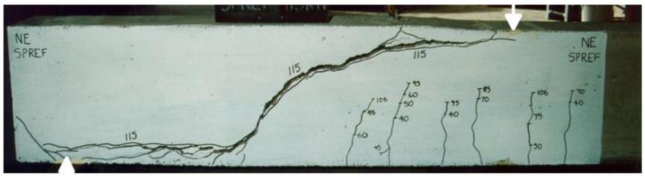

Fig. 5 Shear failure of beam without stirrups (Lucas 2011)

longitudinal reinforcement between one stirrup and the other, as well as the action of the tension of grip τ_b, between the bar and the concrete.

An example of shear failure in a beam without stirrups is shown in Fig. 5. The concrete component of the shear capacity V_c is one of the most intractable problems in reinforced concrete, and extensive experimental testing has been required to develop empirical models to ensure safe design. An example (AS 3600) is shown in the following Eq. (1).

$$V_c = \left(1.4 - \frac{d}{2000}\right)\left(\frac{2d}{a}\right)(bd)\left[\frac{(A_{st} f)_c}{bd}\right]^{1/3} \tag{1}$$

where d and b are the effective depth and width of a beam respectively, a the shear span, and A_{st} the area of the longitudinal reinforcing bars. The lack of understanding surrounding the structural mechanics behind the extremely complex problem of shear failure is reflected in the need for a size effect, as the first parameter, a dimensionally incorrect stress component of the fourth parameter, and the use of lower bounds to represent the design strengths.

The behavior of the concrete wedges can be derived from Mattock and Hawkins' shear-friction theory (Mattock and Hawkins 1972). For a given wedge depth $d_{soft,}$ and from shear friction theory (Oehlers *et al.* 2008), the force the wedge can resist is given by the following equation X.

$$P_{soft} = w_b d_{soft}\left[\frac{c + \sigma_{lat}\cos\alpha(\sin\alpha + m\cos\alpha)}{\sin\alpha(\cos\alpha - m\sin\alpha)}\right] \tag{2}$$

where w_b is the width of the wedge, which is generally the width of the beam, σ_{lat} is the lateral confinement which can be induced by the wrap or by the stirrups, m and c are the shear friction material properties, and α is the angle of the weakest plane which is given by Eq. (3).

$$\alpha = \arctan\left(-m + \sqrt{m^2 + 1}\right) \tag{3}$$

2.2 Manufacture of test specimens and experimental arrangement

For this study, ten specimens of reinforced concrete prismatic beams were made in the following configurations: i) welded reinforcement ii) conventional reinforcement. The models were experimentally tested using the 100-tonne universal testing machine available at LABMAT-Civil Engineering Materials Laboratory at the Federal University of Itajubá.

To obtain the test specimens, both the welded and lashed frames were initially constructed according to the ABNT

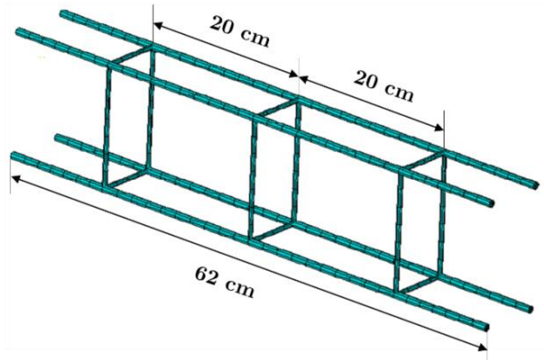

(a)

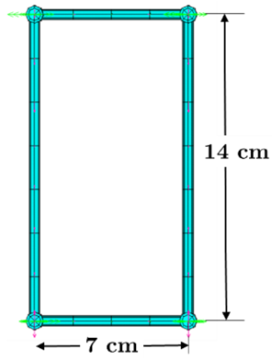

(b)

Fig. 6 Dimensions of the assembled frame (a) and stirrups (b)

Fig. 7 Frame within the forms for the production of beams

NBR 6118 standard. The type of frame used in this study adheres to the definition of passive reinforcement. This refers to a type of reinforcement that is not used to produce pre-tensioning forces, in other words, one that can be pre-stretched (BASTOS 2015). The reinforcement is made up of steel bars, which have the following diameters: (i) 5/16 (8 mm) inches for hardware, and (ii) 3/16 (4.2 mm) inches for stirrups. Fig. 6 details of the types of frames used.

The specimens shown in Fig. 7 were fabricated from wood molds measuring 10×18×65 cm in internal dimension, the desired geometry of the reinforced concrete prismatic beams. Spacers were placed to ensure a minimum spacing of 15 mm along the width of the beam, so that there was no contact between the frame (hardware) and the wood frame. It should be noted that the samples have been reduced in size relative to NBR 12142, due to the fact that they were assembled to fit into test equipment that does not support the relative dimensions set forth in NBR 12142. It is also with noting that this scaling change does not affect

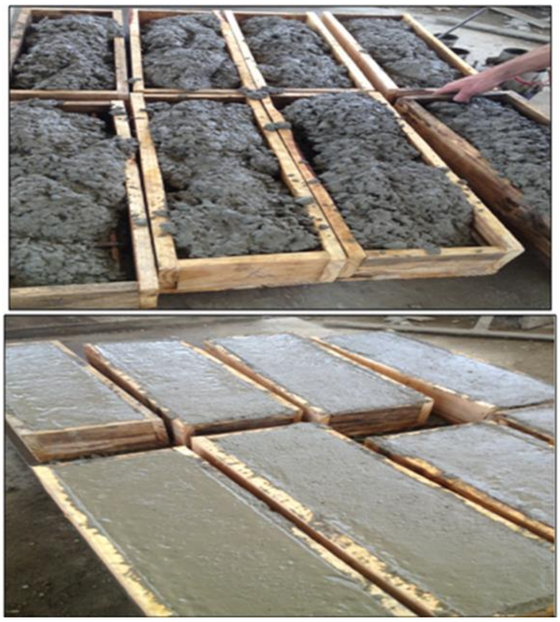

Fig. 8 Completion of the test specimens

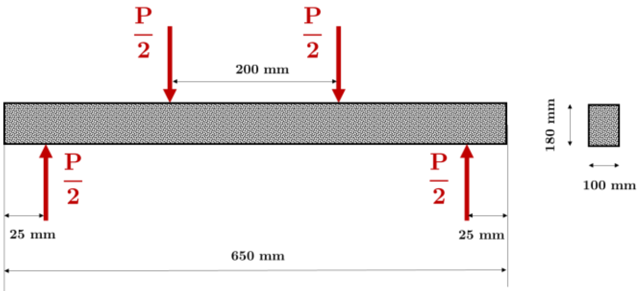

Fig. 9 Configuration of the four point bending test used

the test results.

Subsequently, ABNT NBR 6118 specifies that reinforced filling and densification must be carried out by vibration, centrifugation, or pressing for concrete beams with widths less than 12 cm. More than one of these methods were used to complete the forms with cp5 concrete of 25 MPa linear modulus elasticity that was provided by a construction company. This is shown in Fig. 8. All this was done in compliance with all standards, including the use of spacers between the hardware and the concrete cover. To acquire resistance the concrete beams were cured over a period of 28 days with water for drying.

The type of test performed was a 4-point flexural test, as was previously explained in item 2.12. This consisted of the application of an incrementally increasing load on certain points of the beam. The points of application of the load were located at 200 mm on each side, measured from the position on the *x* axis of the center of the same face, with the supports 25 mm from each end, and with the height as shown Fig. 9. A universal testing machine, belonging to the civil engineering laboratory of the Federal University of Itajubá, was used for the 4-point flexural test. Fig. 10 shows the test subject set into to the test equipment.

Before starting the tests a calibration and adjustment test was performed on the equipment. The universal testing machine can perform various types of mechanical tests such

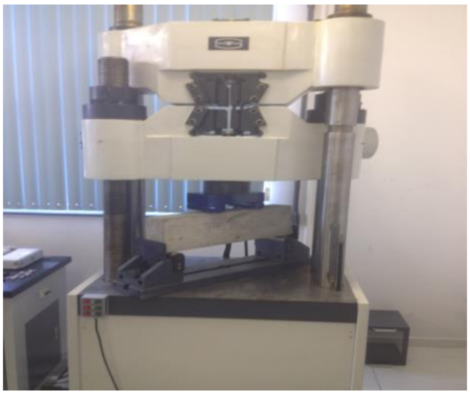

Fig. 10 Probe set into to the universal test machine used in the 4-point assays of the prismatic beams

as: traction, compression, shearing, bending, etc. For this study load tests of up to 100 tones were used. The test can exert several force factors, such as vertical force and tensile/flexural modulus. These various force factors are necessary to carry out the experiments on the beams with bound stirrups and solders, as proposed by this study

2.3 Numerical analysis of strengthened concrete beams

For numerical analysis, the use of ANSYS® software was necessary for the non-linear analysis. Due to the nature of the load application, this study defines the performed analysis as being static structural analysis in nature. The main objective of this type of analysis is to quantify the magnitude of the internal stresses and displacements that occur in the beam and reinforced concrete. Therefore, the effect of damping forces and forces of inertia will be neglected.

Some assumptions in the numerical modeling were carried out, being: i) it was assumed that there was no friction between the test brackets and the piece (beam). That is, the beam could easily slide along the *x* axis (horizontally). This causes the maximum deflection modeled to actually be slightly larger than the actual deflection; ii) the cohesion of the internal steel frame was perfect, that is, one piece and iii) no contact was made between the steel frame and the concrete, the contact between them was assumed to be perfect.

According to Dawari and Vesmawala (2014), there are several engineering computational programs that perform functions of simulations in models based on finite elements, and that have generated highly satisfactory results, in turn reducing the need for large numbers of experiments. An element with the following characteristics was chosen for the simulation of the beams without a frame in finite elements: 8 nodes elements, 3 degrees of freedom per node (translations along the *x*, *y*, and *z* axes).

An element with these characteristics was chosen taking the number of degrees of total freedom of the structure into account, as well as the respective computational demands. Another important property of the element was the ability to simulate the concrete's cracking behavior in traction, and its crushing behavior in compression.

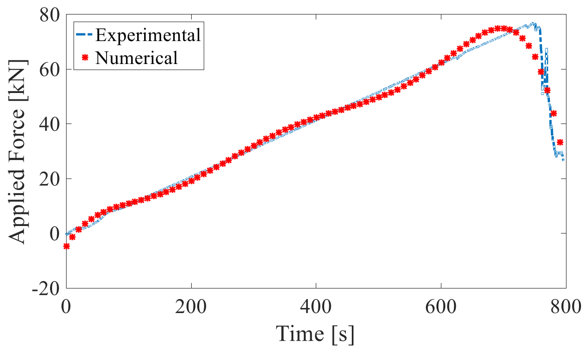

Fig. 11 Numerical and experimental applied load versus time

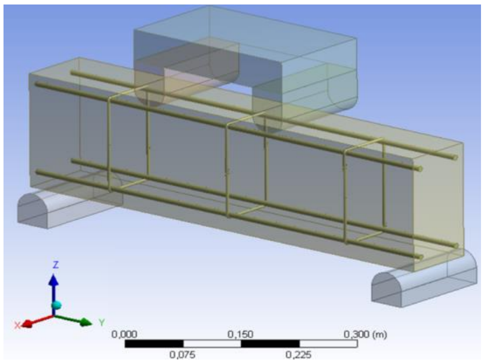

Fig. 12 Numerical model of the beam for FEA and experimental tests

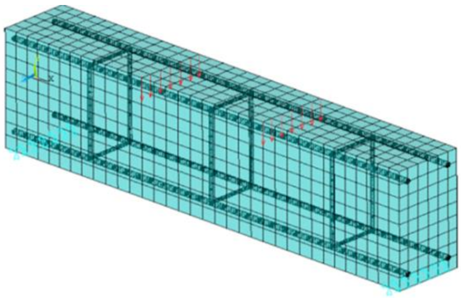

Fig. 13 Discretization of reinforced concrete beam model with frame

It is important to consider the cracking of the concrete, because this cracking is responsible for most of the resultant flaws in this type of fragile material. To simulate the welded frame (hardware and stirrups) a quadratic beam element based on Timoshenko beam theory was used, with the following characteristics: 5 nodes elements, 6 degrees of freedom per node (translations and rotations along the *x*, *y* and *z* axes).

The choice of this type of element was due to the fact that it allowed for different forms of cross sections, using a circular section to represent the hardware and stirrups. The material model for the steel frame was modeled as linear isotropic. It should be noted that both the concrete and the frame were discretized separately, but in such a way as to match the nodes of each one at the interface between them, allowing the components to be coupled.

The load was applied incrementally over time. The data collected by the universal testing machine were taken, and a polynomial regression was performed in order to approximate the numerical simulation as much as possible to the experimental test. The regression equation describing the load is shown in Eq. (4), and the experimental and numerical load-time curves are shown in Fig. 11.

$$\begin{aligned} Force(N) = f(t) = -3.20\times10^{-14}\times t^6 + 6.95\times10^{-11} \\ \times t^5 - 5.60\times10^{-8}\times t^4 + ...2.10\times10^{-5}\times t^3 - 3.69\times10^{-3} \\ \times t^2 + 0.36\times t^6 \end{aligned} \tag{4}$$

As was mentioned before, the frame (hardware and stirrups) was discretized with one element model, and the concrete beam with different model. Thus, a model of material composed of a linear isotropic part and a non-linear part is obtained. For the numerical simulations, the following values in Table 1 were used for both the concrete and the frame parameters.

The mesh of the system was defined by tetrahedral elements of 2 mm in length. The boundary conditions applied to the supports restrict the degrees of freedom: i) displacement *y* and *z* and ii) rotations in *x* and *y*, leaving the set of supports free to move along the *x* axis, and to rotate around *z*.

Due to the fact that the blades and rollers used in the experimental tests have cylindrical ends, it is assumed that the point of contact between these and the reinforced concrete beam is in turn formed by a line composed by the nodes whose constraints have been specified. Fig. 12 illustrates the physical configuration of the assay assembly by means of the blades and rollers of the universal testing machine of the same dimensions as the models assembled for the experimental tests, and Fig. 13 provides a view of the mesh model, constraints, and the model used in this study.

Table 1 Concrete and steel frame properties

Property	Concrete	Frame + Stirrups
Density (kg/m^3)	2400.00	7850.00
Young modulus (GPa)	25.00	210.00
Poisson coefficient	0.20	0.30

3. Numerical and experimental results

The main objective of this study is to compare the behavior of reinforced concrete beams with both welded and tied frames. Additionally, this study intends to numerically simulate the behavior of the welded frame structure via finite elements, so that the behavior of the structure can be understood well before its eventual manufacture. This section shows the different numerical simulations and experimental tests that were used in this study, as well as a discussion of the obtained results.

Ten different samples were constructed for the experimental tests, half of them with welded frames and the other half with tied frames. The results will be presented and discussed below.

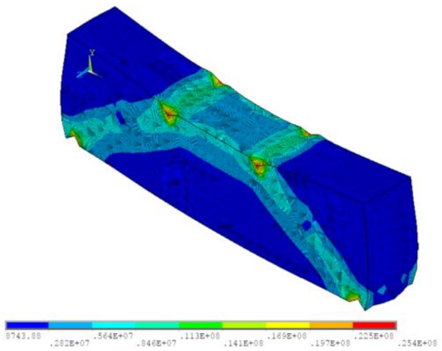

Fig. 14 Von-Mises stress distribution in the concrete beam considering welded stirrup

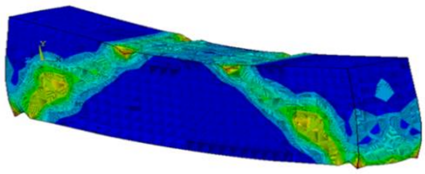

(a)

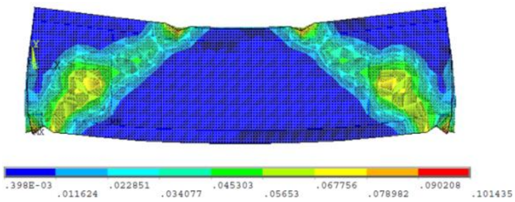

(b)

Fig. 15 Total nodal strain of the studied beam

3.1 Numerical results

In this section the results of the numerical simulations for the reinforced concrete beams are presented. The physical properties of the concrete and structural steel used for the simulations are presented in Table 1. Due to the complexity of modeling the annealed wire ropes, it was decided that simulation should be carried out only for the beams with welded frames, placing the fixed stirrups in the horizontal bars.

Fig. 14 shows the distribution of the Von-Mises stress along the reinforced concrete beam. The numerical rupture stress was expected to be maximum at the supports and points of application of the loads being 25.40 MPa, relatively close to the mean value of the experimental tensile stress of 19.81±2.64 MPa. The proximity of the results shows that there is a relation between the numerical and experimental models, which was the objective of this study.

The distribution of total deformation in the elements composing the reinforced concrete beam is shown in Fig. 15. It was noticed that greater deformations occur along the path between the points of application of the load and the supports, as was observed in the experimental test. Figs. 15 and 16 illustrate the vertical displacement of the beam along the *x* axis, showing that the points of application of the load were those that experienced the greatest negative vertical displacement, and whose maximum value corresponds to

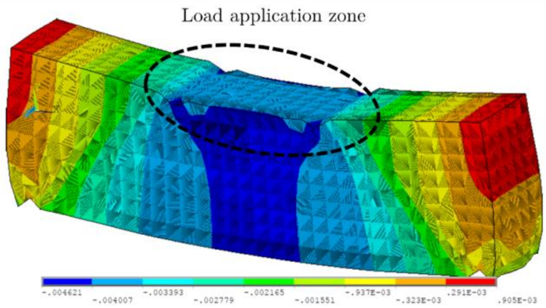

Fig. 16 Vertical nodal displacement of the concrete beam with welded stirrups

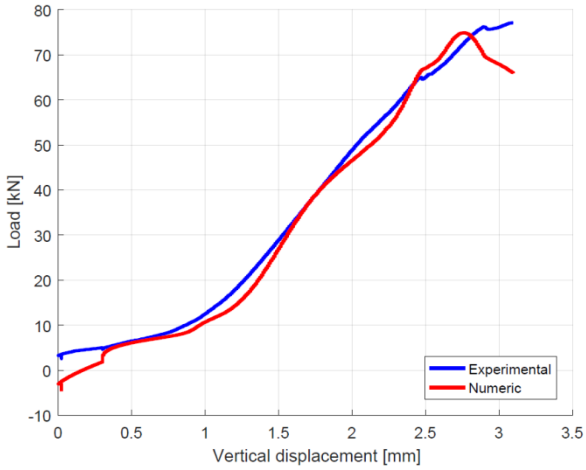

Fig. 17 Vertical nodal displacement along the length of the concrete beam with welded stirrups

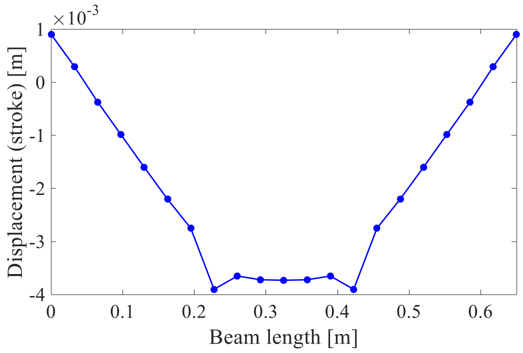

Fig. 18 Vertical nodal displacement along the length of the concrete beam with welded stirrups

approximately -0.0039 m. Analyzing the curves of the Fig. 17, it can be see that the experimental one is more realistic because the initial displacement happens only after a certain load has been applied. In the numerical curve, due to the numerical regression (fitting) made to approximate the numerical load to the experimental test, it generated a small error in which at time t=0 it seems that a negative charge is being applied which is not true, but necessarily in the ANSYS® software. The numerical model was very consistent with the experimental results. Finally, a numerical error due to the approximation of the load vs. time (Figure after Eq. (4) of the article) led to this difference in t=0 between the two curves. Regarding the

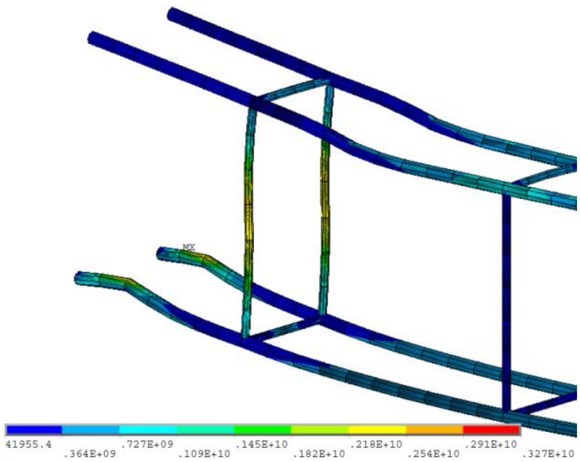

Fig. 19 Von-Mises stress distribution of the welded stirrup concrete beam

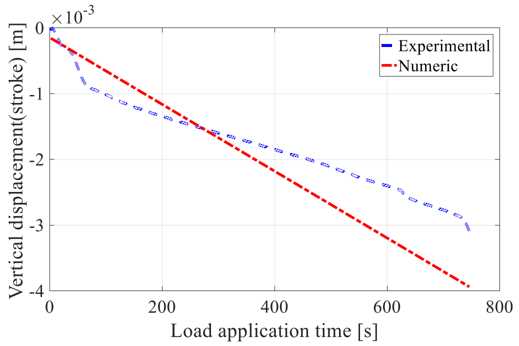

Fig. 20 Comparison of the vertical displacement of the load application point to a welded reinforced stirrup concrete beam

deformation along the *x* axis seen in Fig. 18, specifically at the point of application of the loads, the deformations in that region are around -0.004 m.

In order to demonstrate load transfer from the concrete to the welded steel frame, the Von-Mises voltages acting on both the top and bottom of the frame are shown in Fig. 19. One can observe that the lower fittings are subjected to higher stress distributions than the upper ones, because of the concrete's greater capacity to withstand compressive loads, which protects the frame at the top. It can also be verified that both iron and stirrups would have failed due to the high voltages (values higher than 600 MPa).

Fig. 20 presents a comparison between the numerical and experimental results when analyzing the evolution of the vertical displacement, at the point of the load application, as a function of time. One may observe in Fig. 19 that some correspondence in the evolution of the values exists, albeit with some divergence in the final displacement at the moment of rupture. This divergence can be attributed to the conditions under which both analyses were made.

Thus, the vertical displacement measured by the universal testing machine corresponds exactly to the displacement of the load application, while with the numerical analysis the displacement of the load node (which was initially in contact with the cutlass in addition to the vertical displacement) experienced a slight horizontal displacement due to displacement on the *x*-axis.

3.2 Experimental results

Using the procedures described above, the 10 samples of reinforced concrete, with both welded and attached frames, were tested until they ruptured in order to obtain the results.

After the curing process (28 days) samples were identified. Samples 1 to 5 were the beams that had tied frames, and samples 6 to 10 were beams with welded frames. The following figures detail the results of the experiment. A discussion and summary of the obtained data will be presented in the next chapters.

Fig. 21 shows the final state of the reinforced concrete beams after rupture. Fig. 21(a) shows 45° character cracks, typical of bending tests on concrete prismatic bodies. Fig. 21(b), like the previous figure, also shows 45° character

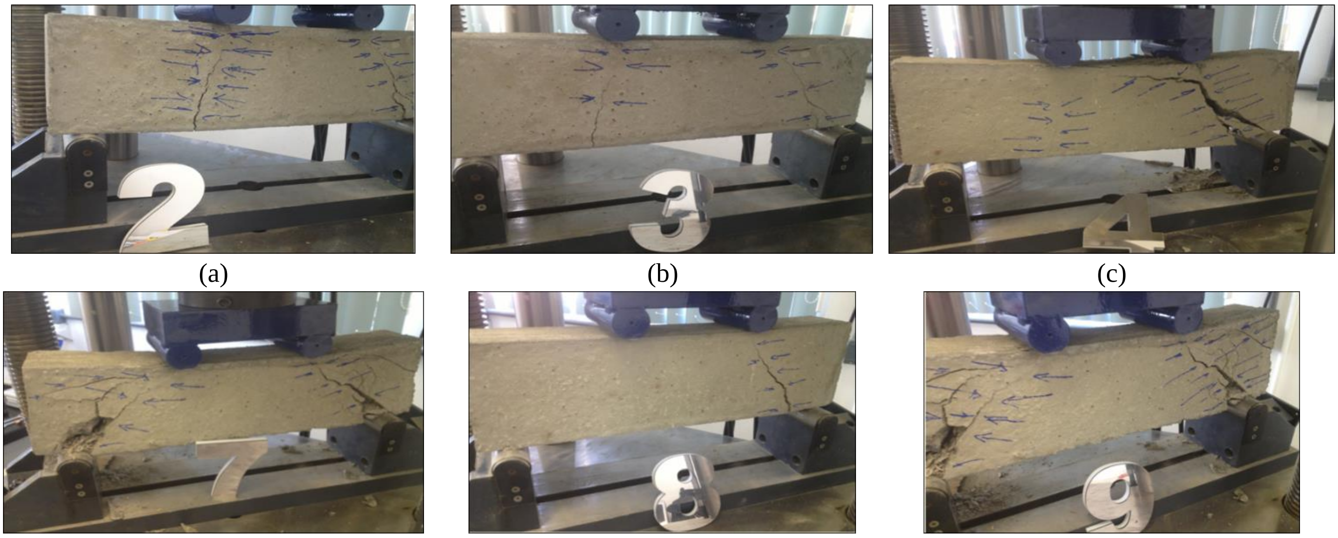

(a) (b) (c)

(d) (e) (f)

Fig. 21 Concrete beam with conventional frames (a, b, c) and welded frames (d, e, f)

Table 2 Stress and failure load of concrete samples

	Failure stress (MPa)		Force (kN)	
	Conventional stirrups	Welded stirrups	Conventional stirrups	Welded stirrups
1	21.19	17.24	70.40	77.30
2	17.40	17.15	74.80	69.65
3	16.83	23.20	77.45	77.10
4	24.66	20.06	81.95	66.65
5	23.10	21.40	78.15	73.80
μ	20.64	19.81	76.55	72.90
σ	3.45	2.64	4.28	4.68

(a)

(b)

(c)

Fig. 22 Concrete beam with welded stirrup (a), (c) and conventional stirrup (b) after the failure

cracks, typical of flexural tests on concrete prismatic bodies. Fig. 21(c) similarly exhibits characteristics of 45° cracks, typical of tests of bending on prismatic bodies of concrete, however, larger cracks were observed on the right side. Similarly, Figs. 21(d), 21(e), and 21(f) show the final after rupture state of the reinforced concrete beams with welded frames. Like the previous figures, Fig. 21(d) shows 45° character cracks, typical of bending tests on concrete prismatic bodies. In Fig. 21(e), the cracks begin on the right side with a 45° crack, also typical of bending tests on concrete prismatic bodies. In Fig. 21(f), 45° cracks occurred, i.e., a very typical failure of concrete test bodies.

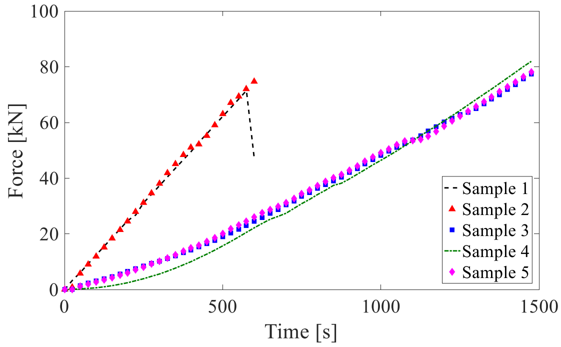

Fig. 23 Numerical and experimental force results for the beam with conventional stirrups

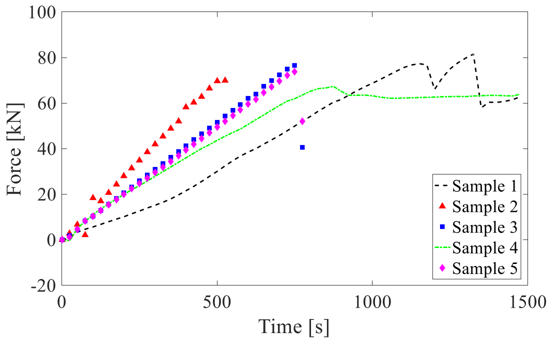

Fig. 24 Numerical and experimental force results for the beam with welded stirrups

The following data was obtained during from tests: i) the evolution of the applied load as a function of time, ii) the modulus or rupture stress, iii) the deformation, and lastly iv) the test time. The results of the modulus and rupture loads of the 10 tested samples are given in Table 2.

As a result of the rupture of the samples tested, the details of the welded and tied frame in the region of the rupture are shown in Fig. 22(a) and Fig. 22(b) respectively. Fig. 22(c) shows that the stirrups broke in the location of the weld due to the acting forces, this effect also owing itself to the contribution of the electrode applied at that location.

Figs. 23 and 24 show the load curves applied as a function of time for the beams with tied and welded frames respectively. The end point of the curve corresponds to the rupture point.

4. Conclusions

This study sought to perform experimental tests and to implement a numerical model that allowed for the calculation of the structural behavior of reinforced concrete beams in two configurations: i) with welded frames and ii) with tied frames using annealed steel wire.

Loads were applied to the beams until they ruptured in accordance with the standards set forth for a 4-point bending test, and both the modulus of rupture, and the loads at which the failure occurred were measured. In an attempt to reduce the number of future experiments, it was decided that a numerical model should be developed in order to verify the experimental tests.

The literature review identified a general lack of research on the issue of welded reinforcements in the design of prismatic beams. In most cases, welded frames are used to coat concrete floors, which do not withstand heavy bending stresses on prismatic building beams in general terms. The advantages of welded reinforcement, from a factory point of view, outweigh those of in situ fittings, due to the ease and time of preparation. This depends, however, on intended use and the type of work to be undertaken, as there are without doubt certain limitations.

One may concluded that, in general, according to the statistical data, the configurations of both welded and tied frames showed very similar structural performances when considering the load and modulus of the rupture. The following aspects may be mentioned based on observation and the numerical results:

• One may observe that the beams with welded frames, in samples 07 and 09, showed stirrup breakage at the weld at the maximum peak of force. This was due to the applied electrode at that particular location. There was no break or violation of the wires at the mooring point in the beams with mooring.

• While taking a more detailed analysis of the data obtained in the experimental tests into account, the beams with tied frames supported a relatively higher stress on average, and consequently, the tensile strength was also higher. This is attributed to the greater flexibility of the frame resulting from the ties, whereas a more rigid structure, such as the welded frame, would have generated greater forces in the concrete-steel frame, consequently leading to the rupture of the stirrups.

• As seen in Deivanai and Sathia (2016), the ultimate load on average for tied stirrups reinforcement was lower than the welded one, in conjunction with the previous remark is easy to see that more energy in necessary to achieve the maximum tensile strength in tied frames but the rigidity of the welded structure offers higher resistance.

• The numerical analysis showed that the steel frame absorbed the greatest tensile stresses. However, is already well known that concrete cracking occurs initially in the traction region.

• Given the differences between the numerical and experimental tests, it was shown that there was very little relative difference in the final value of the vertical displacement (U_Y). However, this may be due to the failure to consider the experimental U_X measurement of the beam over the test time, given the absence of constraints along this axis. This resulted in a very similar numerical and experimental mode of rupture. This fact encourages the use of FEM simulations in the study of reinforced concrete structures without the need for experiments.

Acknowledgments

The authors would like to acknowledge the financial support of the Brazilian agency CNPq-(National Council for Scientific and Technological Development) and CAPES-(Coordination for the Refinement of Students of Higher Education).

References

Alam, M. and Hussein, A. (2012), "Size effect on shear strength of FRP reinforced concrete beams without stirrups", *J. Compos. Constr.*, **17**(4), 507-516.

Altunişik, A.C., Bayraktar, A. and Sevim, B. (2013), "Analytical and experimental modal analyses of a highway bridge model", *Comput. Concrete*, **12**(6) 803-818.

Azad, A., Mirza, M. and Chan, P. (1989), "Fracture energy of weakly reinforced concrete beams", *Fatig. Fract. Eng. Mater. Struct.*, **12**(1), 9-18.

Bastos, P.S.D.S. (2008), *Dimensionamento de Vigas de Concreto Armado à Força Cortante*, UNESP, São Paulo.

Colajanni, P., Mendola, L., Mancini, G., Recupero, A. and Spinella, N. (2014), "Shear capacity in concrete beams reinforced by stirrups with two different inclinations", *Eng. Struct.*, **81**, 444-453.

Colajanni, P., Recupero, A. and Spinella, N. (2014), "Design procedure for prestressed concrete beams", *Comput. Concrete*, **13**(2), 235-253.

Colajanni, P., Recupero, A. and Spinella, N. (2014), "Design procedure for prestressed concrete beams", *Comput. Concrete*, **13**(2), 235-253.

Collins, M.P., Mitchell, D., Adebar, P.E. and Vecchio, F.J. (1996), "A general shear design method", *ACI Struct. J.*, **93**(1), 36-45.

Cosgun, T. and Sayin, B. (2014), "A method for the non-linear and failure load analysis of reinforced concrete frames", *Comput. Concrete*, **14**(1), 41-57.

Dawari, V.B. and Vesmawala, G.R. (2014), "Application of nonlinear concrete model for finite element analysis of reinforced concrete beams", *Int. J. Scientif. Eng. Res.*, **5**(9), 776-782.

Deivanai, R. and Sathia, R. (2016), "A comparative study of welded and tied shear reinforcement in beams", *J. Chem. Pharmaceut. Sci.*, **9**(3), 1535-1537.

Fan, X.Q. and Hu, S.W. (2013), "Influence of crack initiation length on fracture behaviors of reinforced concrete", *Appl. Clay Sci.*, **79**, 25-29

Ferro, G., Carpinteri, A. and Ventura, G. (2007), "Minimum reinforcement in concrete structures and material structural instability", *Int. J. Fract.*, **146**(4), 213-231.

Fiorin, E. (1998), "Arranjos de armaduras em estruturas de concreto armado", Doctoral Dissertation, Universidade de São Paulo, São Carlos, SP.

Fusco, P.B. (1995), *Técnica de Armar as Estruturas de Concreto*, Pini.

Fusco, P.B. (2000), *Estruturas de Concreto: Solicitações Normais, Estados Limites Últimos*, Teoria e Aplicações, Rio de Janeiro, LTC, c1981. 464, ISBN 85-216-1143-9.

Giongo, J.S. (2005), *Concreto Armado: Projeto Estrutural de Edifícios*, EESC/SET.

Gursoy, S. (2014), "Investigation of nonlinear behaviour of reinforced concrete frames having different stiffening members", *Comput. Concrete*, **13**(5), 679-694.

Haifeng, L. and Jianguo, N. (2009), "Mechanical behavior of reinforced concrete subjected to impact loading", *Mech. Mater.*, **41**, 1298-1308

Han, J., Cai, Y., Lin, C., Gao, G. and Wang, F. (2011), "Experimental research on seismic behavior of unbonded precast reinforced concrete frame", *Syst. Eng. Procedia*, **1**, 137-

141
Hossain, T. and Okeil, A.M. (2014), "Force transfer mechanism in positive moment continuity details for prestressed concrete girder bridges", *Comput. Concrete*, **14**(2), 109-125.
Hu, S.W., Lu, J. and Zhong, X. (2011), "Study on characteristics of acoustic emission property in the normal concrete fracture test", *Adv. Mater. Res.*, **189-193**, 1117-1121.
Ibraheem, O.F., Abu, B. and Johari, I. (2014), "Fiber reinforced concrete L-beams under combined loading", *Comput. Concrete*, **14**(1), 1-18.
Javidan, F., Shahbeyk, S. and Safarnejad, M. (2014), "Lattice discrete particle modeling of compressive failure in hollow concrete blocks", *Comput. Concrete*, **13**(4), 437-456.
Ju, Y.K., Kim, J.Y. and Kim, S.D. (2007), "Experimental evaluation of new concrete encased steel composite beam to steel column joint", *J. Struct. Eng.*, **133**(4), 519-529.
Kaefer, L.F. (1998), *A Evolução do Concreto Armado*, São Paulo, 43.
Kaklauskas, G. and Ghaboussi, J. (2001), "Stress-strain relations for cracked tensile concrete from RC beam tests", *J. Struct. Eng*., **127**(1), 64-73.
Khan, M., Fahad, M. and Shahzada, K. (2015), "Shear capacity of reinforced concrete beams using swimmer bars as shear reinforcement", *Int. J. Civil Eng*., **2**(6), 20-26.
Leonhardt, F. and Mönnig, E. (1977), "Construções de concreto: princípios básicos do dimensionamento de estruturas de concreto armado", *Interciência*, **1**, Rio de Janeiro.
Lin, X., Zhang, Y.X. and Hazell, P.J. (2014), "Modelling the response of reinforced concrete panels under blast loading", *Mater. Des.*, **56**, 620-628
Lucas, W.D. (2011), "The discrete rotation behaviour of reinforced concrete beams under shear loading", Doctoral Dissertation.
Lykidis, G.C. and Spiliopoulos, K.V. (2014), "An efficient numerical simulation of the cyclic loading experiments on RC structures", *Comput. Concrete*, **13**(3), 343-359.
Markou, G. and Papadrakakis, M. (2013), "Computationally efficient 3D finite element modeling of RC structures", *Comput. Concrete*, **12**(4), 443-498.
Marzec, I., Skarzynski, L., Bobinski, J. and Tejchman, J. (2013), "Modelling reinforced concrete beams under mixed shear-tension failure with different continuous FE approaches", *Comput. Concrete*, **12**(5), 585-612.
Mattock, A.H. and Hawkins, N.M. (1972), "Shear transfer in reinforced concrete-Recent research", *PCI J.*, **17**(2), 55-75.
Mosoarcam, M. and Victorm, G. (2013), "Structural safety of historical buildings made of reinforced concrete, from Banat region- Romania", *J. Cult. Heritage*, **14**, e29-e34.
Nielsen, M.P. (1984), *Limit Analysis and Concrete Plasticity*, Prentice-Hall, Englewood Cliffs, NJ.
Oehlers, D.J., Ali, M.M. and Griffith, M.C. (2008), "Concrete component of the rotational ductility of reinforced concrete flexural members", *Adv. Struct. Eng.*, **11**(3), 281-291.
Rosso, T. (1980), *Racionalização da Construção*, FAUUSP, São Paulo.
Ruiz, G., Elices, M. and Planas, J. (1998), "Experimental study of fracture of lightly reinforced concrete beams", *Mater. Struct.*, **31**(214), 683-691.
Russo, G. and Puleri, G. (1997), "Stirrup effectiveness in reinforced concrete beams under flexure and shear", *ACI Struct. J.*, **94**(3), 451-476.
Russo, G., Somma, G. and Angeli, P. (2004), "Design shear strength formula for high strength concrete beams", *Mater. Struct*., **37**(274), 680-688.
Russo, G., Venier, R. and Pauletta, M. (2005), "Reinforced concrete deep beams-shear strength model and design formula", *ACI Struct. J*., **102**(3), 429-437.
Saw, H.A., Villaescusa, E., Windsor, C.R. and Thompson, A.G. (2017), "Surface support capabilities of freshly sprayed fibre reinforced concrete and safe re-entry time for underground excavations", *Tunnel. Underg. Space Technol.*, **64**, 34-42
Shatarat, N., Katkhuda, H., Abdel-Jaber, M. and Alqam, M. (2016), "Experimental investigation of reinforced concrete beams with spiral reinforcement concrete beams with spiral reinforcement in shear", *Constr. Build. Mater*., **125**, 585-594.
Shedeh, G. (2015), "Beam shear analysis of concrete with fiber-reinforcement plastic", *Int. J. Res. Civil Eng.*, **3**(1), 7-20.
Silva, R.C.D. (2003), "Vigas de concreto armado com telas soldadas: análise teórica e experimental da resistência à força cortante e do controle da fissuração", Doctoral Dissertation, Universidade de São Paulo.
Souza, M.D. and Rodrigues, R. (2008), *Sistemas Estruturais de Edificações e Exemplos*, Orientador Dr. Nilson Tadeu Mascia, São Paulo.
Süssekind, J.C. (1977). *Curso de Análise Estrutural-Vol. 2: Deformações em Estruturas, Método das Forças-Vol. 3: Método das Deformações*, Processo de Cross.
Turker, T. and Bayraktar, A. (2014), "Vibration based damage detection in a scaled reinforced concrete building by FE model updating", *Comput. Concrete*, **14**(1), 73-90.
Ulzurrun, G. and Zanuy, C. (2017), "Enhancement of impact performance of reinforced concrete beams without stirrups by adding steel fibers", *Constr. Build. Mater.*, **145**, 166-182.
Vecchio, F.J. and Collins, M.P. (1986), "The modified compression field theory for reinforced concrete elements subjected to shear", *ACI Struct. J.*, **83**(2), 219-231
Xuan, X.Y. (1987), "Effectiveness of welded wire fabric as shear reinforcement in pretensioned prestressed concrete T-beams", A Thesis presented to the University of Manitoba in partiaì fuìfillment of the requi rements for the degree of M.Sc. in the Department of Civil Engineering.
Yelgin, A.N., Özyurt, M.Z. and Uysal, M. (2014), "The structural behaviour of composite beams with prefabricated reinforced concrete plate in positive moment zone", *Constr. Build. Mater.*, **68**, 627-629
Zhou, Z., Wu, C., Meng, S.P. and Wu, J. (2014), "Mechanical analysis for prestressed concrete containment vessels under loss of coolant accident", *Comput. Concrete*, **14**(2), 127-143.
Zhu, H.Y., Deng, J.G., Zhao, J., Zhao, H., Liu, H.L. and Wang, T. (2014), "Cementing failure of the casing-cement-rock interfaces during hydraulic fracturing", *Comput. Concrete*, **14**(1), 91-107.

HK